DLINE JOURNALS

Progress in Signals and Telecommunication Engineering

Print ISSN: 2319-457X
Online ISSN: 2319-4588

PSTE 2024; 13 (2)
https://doi.org/10.6025/pste/2024/13/2/70-77

Designing A Clutter Suppression Algorithm for Synthetic Aperture Radar

Leonid G. Dorosinskiy and Andrew A. Kurganski
Ural Federal University, pr. Mira, 19
Yekaterinburg, 620002, Russian Federation
k-and92@mail.ru

ABSTRACT

Modeling the clutter reflection suppression algorithm in synthetic-aperture radar is considered in the article. The proposed algorithm allows one to increase the signal detection eciency with closely located sources of clutter due to the use of a priori data of static objects of the infrastructure.

Received: 3 March 2024
Revised: 10 June 2024
Accepted: 23 June 2024

Keywords: Optimal Detection Algorithm, SAR, Clutter Suppression

1. Introduction

The forming problem of the optimal algorithm for signal detection in the radar with synthesized aperture (SAR) under the presence of the clutter re ections from the local objects and the design of the efficiency estimation method of such detection are the main problems in the development air and satellite observational platforms for remote earth and water surfaces sensing system.

2. Algorithm Development

Devoted to the problems of signal processing within the SAR papers [1-3] pay great attention to research of the detection algorithms under clutter impact caused by the reflection from the underlying surface and noises. A SAR antenna pattern in some practical situations (along with the valid signal reflected from the multiple-unit target) has powerful clutter signals produced by the reflections from the clutter objects. Therefore, in these cases the processing algorithm should be formed accounting both the distribution target character and the clutter presence. Determination of the main principles of algorithm construction and the analysis methods present the content of this paper. Suppose the side-looking radar moves along the linear path. The range resolution cell has the target and clutter signals formed by the separate reflectors, which are distant at $d_i^t(i=\overline{1,n})$ and $d_i^c(i=\overline{1,N})$ from the coordinate origin with the Δt step, and *n and N* are the numbers of the target and clutter reflectors respectively (Figure 1). Under the discrete time processing, the vector of the observed data is presented in the following form:

$$Y = \beta_{\mathrm{T}} A_{\mathrm{T}} + \beta_{\mathrm{C}} A_{\mathrm{C}} + N_{\mathrm{N}} \tag{1}$$

$$\beta_{\mathrm{T}} = \left\| \begin{matrix} X(d^{\mathrm{t}}_{1,1}), X(d^{\mathrm{t}}_{2,1}), \ldots, X(d^{\mathrm{t}}_{n,1}) \\ X(d^{\mathrm{t}}_{1,2}), X(d^{\mathrm{t}}_{2,2}), \ldots, X(d^{\mathrm{t}}_{n,2}) \\ \cdots \\ X(d^{\mathrm{t}}_{1,M}), X(d^{\mathrm{t}}_{2,M}), \ldots, X(d^{\mathrm{t}}_{n,M}) \end{matrix} \right\| \tag{2}$$

where

$$X(d^{\mathrm{t}}_{n,k}) = \left\| \exp(-j\frac{4\pi}{\lambda R_0} d^{\mathrm{t}}_n r_k) \right\| \tag{3}$$

is the phase signal distribution reflected from i-target element on the points of synthesized aperture with the coordinates $r_k,\ k = \overline{1,M}$ (λ is the wavelength); A_T *and* A_c are (n×1) and (N×1) vectors of complex target and clutter amplitudes which are normal random variables with zero mean and dispersions $\sigma^2_{\mathrm{T}i}$ and $\sigma^2_{\mathrm{C}i}$ respectively; matrix β_{C} is determined similarly to (2) and (3), N_{N} is the complex amplitude vector of gaussian noise.

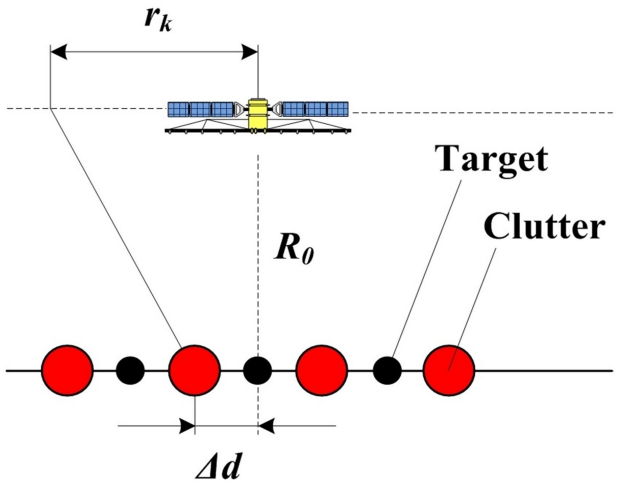

Figure 1. Task geometry

Recording the observed data in the form (1), the quadric form of sufficient statistics for the detection of the target signal is

$$\alpha = Y^{*\mathrm{T}} \theta Y, \tag{4}$$

where $\theta = R_{\mathrm{C}}^{-1} - R_{\mathrm{TC}}^{-1}$ is the processing weight function,

$$R_{\mathrm{TC}} = \beta_{\mathrm{T}} Q_{\mathrm{T}} \beta_{\mathrm{T}}^{*\mathrm{T}} + R_{\mathrm{C}}^{-1}, \tag{5}$$

$$R_{\mathrm{C}} = \beta_{\mathrm{C}} Q_{\mathrm{C}} \beta_{\mathrm{C}}^{*\mathrm{T}} + R_{\mathrm{N}}, \tag{6}$$

are the correlation matrices of vector (1) with and without the target signal respectively

$$Q_{\mathrm{T}} = \mathrm{diag}(\sigma^2_{\mathrm{T}_1}, \ldots, \sigma^2_{\mathrm{T}_n}), \tag{7}$$

$$Q_{\mathrm{C}} = \mathrm{diag}(\sigma^2_{\mathrm{C}_1}, \ldots, \sigma^2_{\mathrm{C}_N}), \tag{8}$$

$$R_{\mathrm{N}} = \sigma^2_{\mathrm{N}} E \tag{9}$$

where * is a complex conjugation, T is a transpose sign, E is the identity matrix with the noise dispersion $\sigma^2_{\mathrm{N}} = 1$. Using Woodbury formula for the determination of the optimal weight function the equation of the sufficient statistics derives as

$$\alpha = ZPZ^{*\mathrm{T}}, \tag{10}$$

where

$$P = (E + Q_{\mathrm{T}}\beta^{*\mathrm{T}}_{\mathrm{T}} R^{-1}_{\mathrm{C}} \beta_{\mathrm{T}})^{-1} Q_{\mathrm{T}}, \tag{11}$$

$$R^{-1}_{\mathrm{C}} = R^{-1}_{\mathrm{N}} - R^{-1}_{\mathrm{N}} \beta_{\mathrm{C}} (E + Q_{\mathrm{C}} \beta^{*\mathrm{T}}_{\mathrm{C}} R^{-1}_{\mathrm{N}} \beta_{\mathrm{C}})^{-1} Q_{\mathrm{C}} \beta^{*\mathrm{T}}_{\mathrm{C}} R^{-1}_{\mathrm{N}}, \tag{12}$$

$$Z = Y^{\mathrm{T}} R^{-1}_{\mathrm{C}} \beta^{*}_{\mathrm{T}} = Y^{\mathrm{T}} X^{*}(d^{\mathrm{t}}_i) - \sum_{l=1}^{N} \chi_{li} Y^{\mathrm{T}} X^{*}(d^{\mathrm{c}}_l), \tag{13}$$

$$\chi_{li} = \sum_{t=1}^{n} \rho_{lt} X^{\mathrm{T}}(d^{\mathrm{c}}_t) X^{*}(d^{\mathrm{c}}_i) \tag{14}$$

where ρ_{lt} It is the matrix (11) element.

The schematic structure with the optimal algorithm (10) is shown on Figure 2.

The main functional operation in (13) is

$$Y^{\mathrm{T}} X^{*}(d_i) = \sum_{k=1}^{M} \exp(-j \frac{4\pi}{\lambda R_0} d^{\mathrm{t}}_i r_k) \tag{15}$$

that presents the chirp demodulation and the discrete Fourier transform (DFT) estimated for the spatial frequencies $2d_i/\lambda R_0$ that corresponding to all elements of target (clutters).

3. Algorithm Analysis

The relative gain of the optimal processing in comparison with the traditional one in SAR does not allow one to estimate the absolute values of the detection characteristics with multiple-unit sources of signals and clutters. On the other hand, the exact calculation of these characteristics is connected with the significant calculation difficulties caused in the determination and integration of distributed statistics (10). Therefore, the efficiency estimation of the considered algorithm uses the method based on the Chernoff bound [3], according to which the detection and false alarm probabilities are counted the formulas

$$P_D = -\exp[\gamma(\nu(s) + (1-s)(\dot{\nu}(s) + 0.5(1-s)^2)\ddot{\nu}(s))] \times \mathrm{erfc}[(1-s)\sqrt{\gamma\ddot{\nu}(s)}], \tag{16}$$

$$P_F = \exp[\gamma(\nu(s) + s\dot{\nu}(s) + 0.5s^2\ddot{\nu}(s))] \times \mathrm{erfc}[s\sqrt{\gamma\ddot{\nu}(s)}], \tag{17}$$

where

$$\nu(s) = \ln \int_{-\infty}^{\infty} \ldots \int_{-\infty}^{\infty} P\left[\left(\frac{Y}{T+C}\right)\right]^2 [P(Y/C)]^{1-s} dY, \tag{18}$$

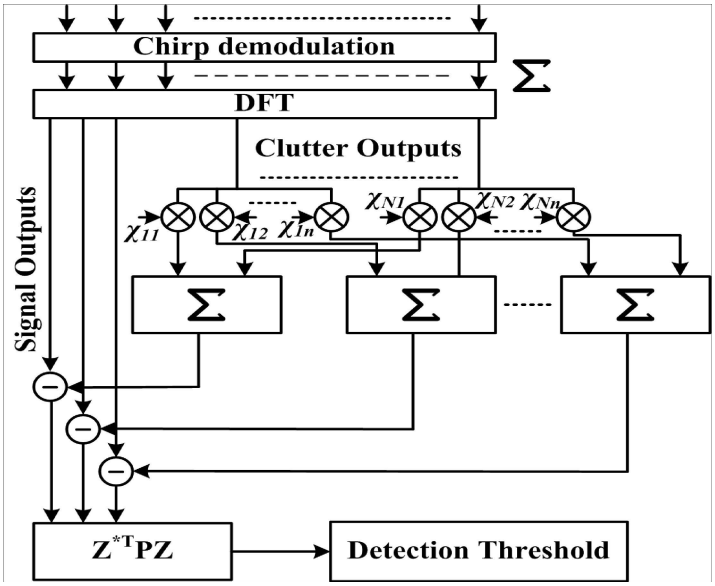

Figure 2. Optimal algorithm flowchart

and $\dot{\nu}(s)$ and $\ddot{\nu}(s)$ are the first and second derivatives of (18), s = 0 ... 1 is the dummy argument, γ is the number of independent tests (for SAR γ is the nlook, e.g. the number of used frequencies with multi frequency probing or the number of non-coherent summed synthesized images for partly coherent SAR working mode), *P(Y=(T + C)); P(Y=C)* are the probability densities of the observed vector under presence or absence of the target signal.

According to the case presented in the paper, formula (18) has the following form:

$$\nu(s) = -0.5 \times \ln(\det(R_{\mathrm{T}}) \times s + \det(R_{\mathrm{C}}) \times (1-s) \\ +0.5s \times \ln(R_{\mathrm{T}}) + 0.5(1-s)\ln(\det(R_{\mathrm{C}})). \qquad (19)$$

Using formulas (16)-(19), the performance and detection characteristics are calculated. The perfomance curves shown in Figure 3-5 are calculated for the case when there is only one target and one clutter, $\sigma_{\mathrm{T}}^2 = \sigma_{\mathrm{C}}^2 = \sigma_{\mathrm{N}}^2 = 1$, and the number of observation periods is M = 1300.

In the graphs, the performance curves are also shown for the no-clutter case and for processing that does not use the algorithm presented in the article.

Figure 3 shows curves for different values of target-clutter space and Δd at γ = 1. The graph shows that processing using the algorithm described in the article improves the detection characteristics even at γ = 1. With increasing target-clutter space, starting from 10 m, the performance curve approaches to the case when the clutter is completely absent.

Figure 4 shows the curves for different values of γ at Δd = 20m. Figure 5 is the zoomed part of Figure 4. With increasing γ, detection characteristics have a significant gain in comparison with processing without clutter compensation.

Detection characteristics of a multi-element target (n = 5) against a background of multiple-element clutter (N = 5) for $(N = 5)$ for $\sigma_{\mathrm{N}}^2 = 1, \sigma_{\mathrm{C}}^2 = \{0.1; 1; 0.1; 0.7; 0.5\}$, M = 100; γ = 2 for different target-clutter location cases (Figure 6) are shown in Figure 7.

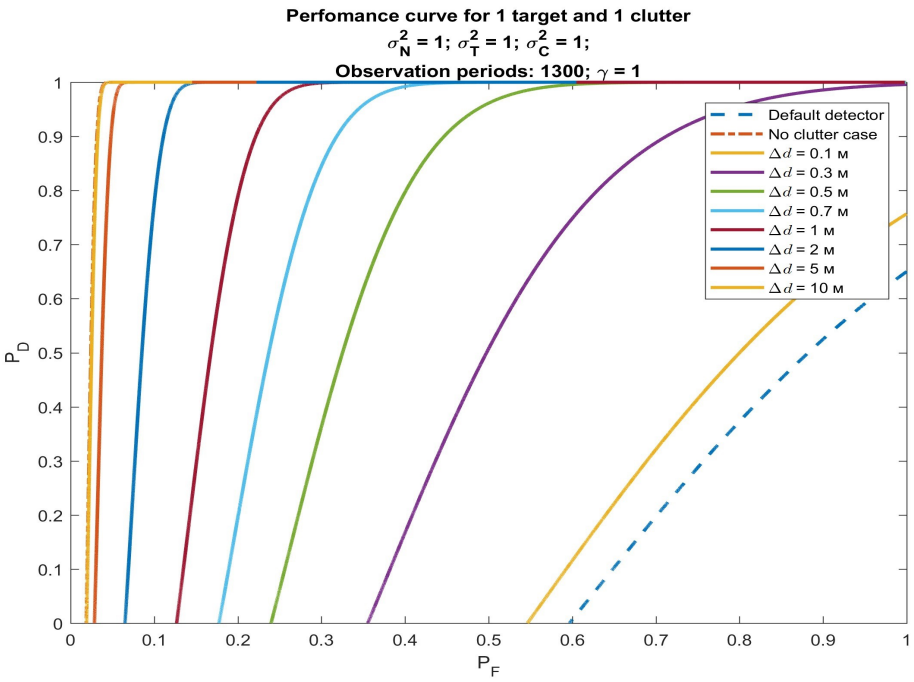

Figure 3. Performance curves for 1 target and 1 clutter

From the presented curves it follows that with a greater spatial separation of the target and clutters the algorithm significantly increases the detection probability of the target.

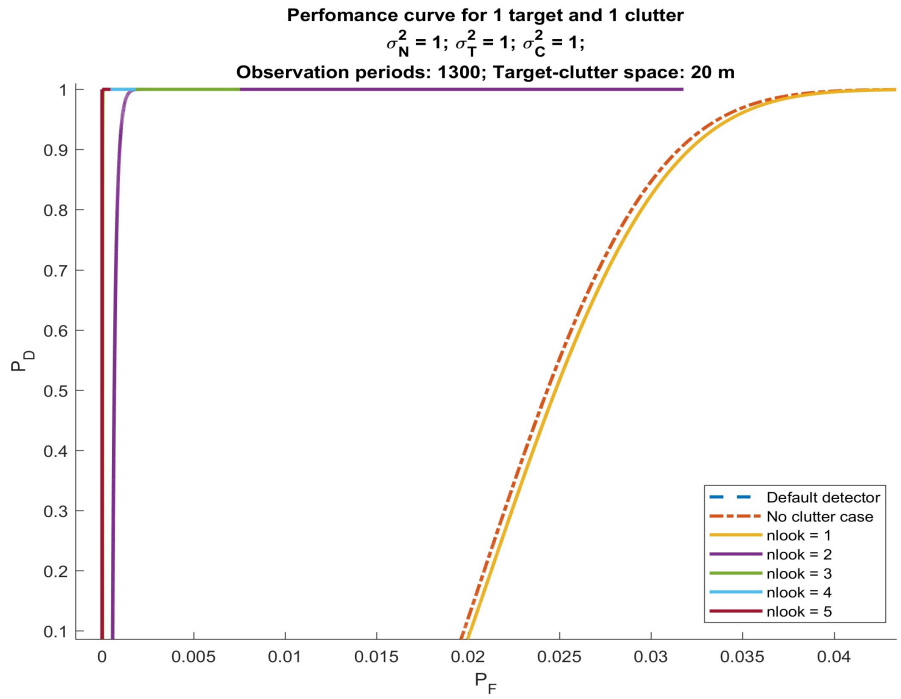

Figure 4. Performance curves for 1 target and 1 clutter

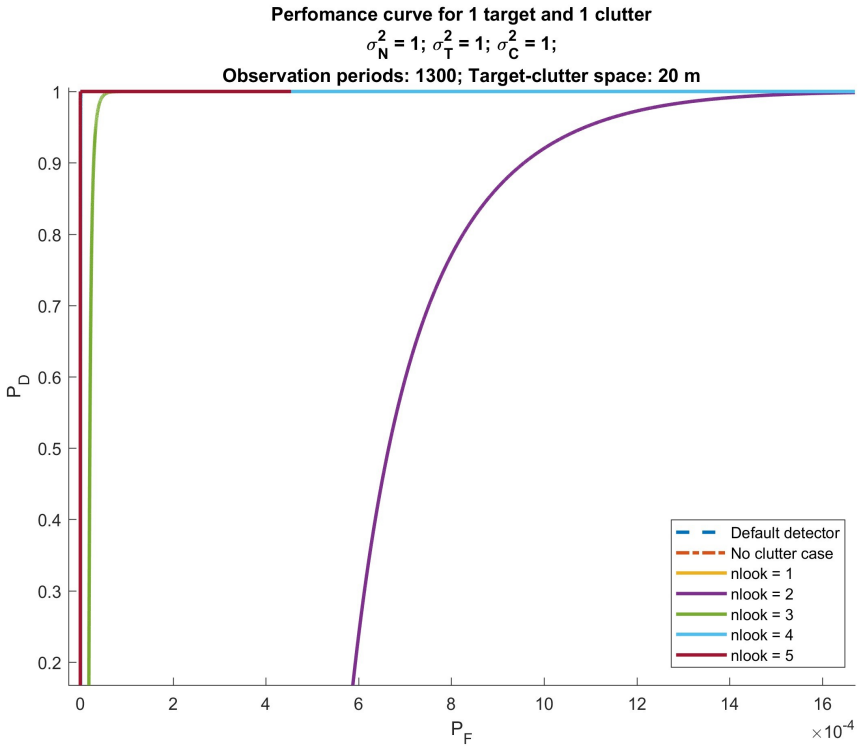

Figure 5. Performance curves for 1 target and 1 clutter (zoomed)

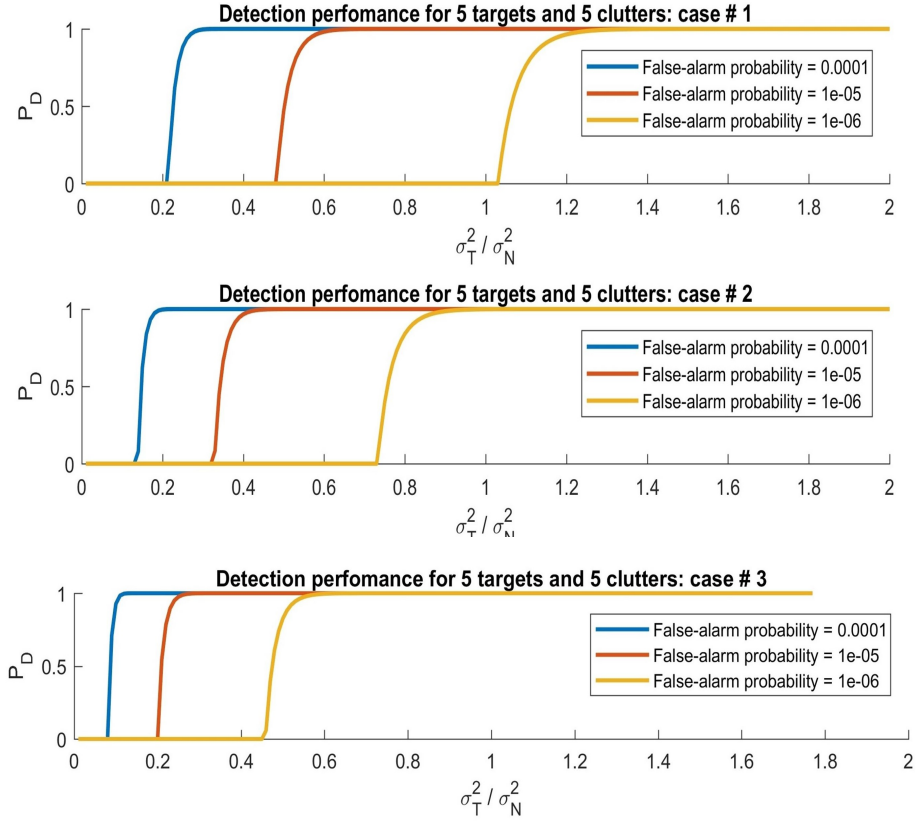

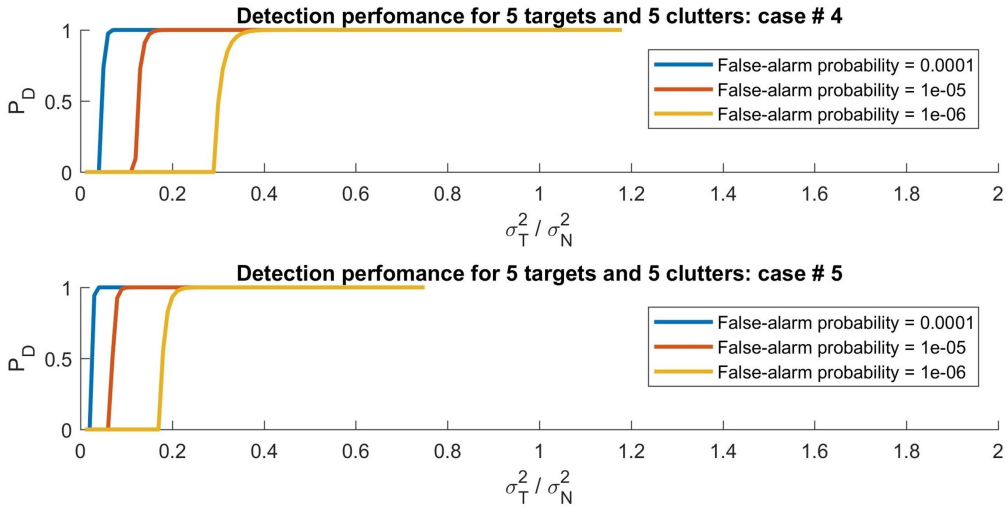

Figure 6. Detection performance for 5 targets and 5 clutters

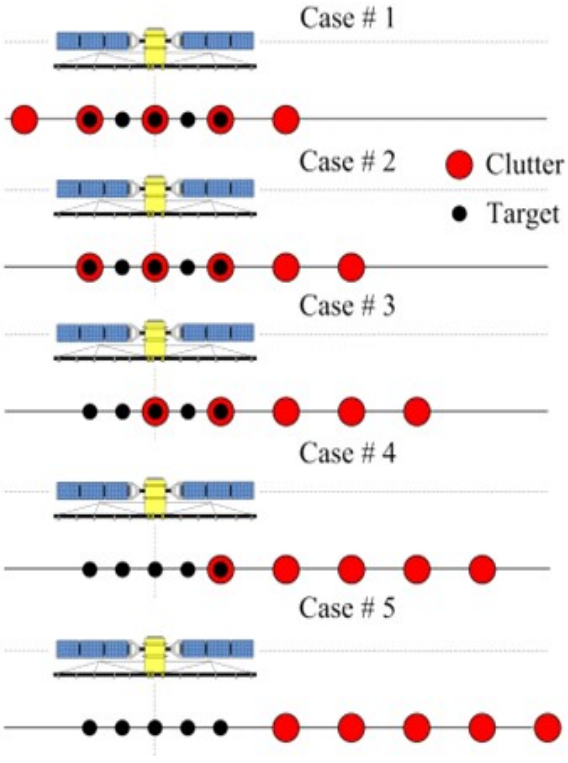

Figure 7. Target-clutter location cases

4. Conclusion

Clutter reflection suppression algorithm in SAR presented in the article significantly improves the detection efficiency of the signals reflected from targets, which are locate red closely with clutter objects, even in cases where the clutters overlap targets.

References

[1] Yang, D., Yang, X., Liao, G. (2015). Strong clutter suppression via RPCA in multichannel SAR/GMTI system. *IEEE Geoscience and Remote Sensing Letters, 12*(11).

[2] Baumgartner, S. V. (2012). Fast GMTI algorithm for traffic monitoring based on a priori knowledge. *IEEE Transactions on Geoscience and Remote Sensing, 50*(11).

[3] Dorosinskiy, L. G. (2013). The research of the distributed objects radar image recognition algorithms. In *Applied and Fundamental Studies: Proceedings of the 2nd International Academic Conference* (Vol. 1, pp. 211–214).